The unequal distribution of water risks and adaptation benefits in coastal Bangladesh

Emily J. Barbour[1,2], Mohammed Sarfaraz Gani Adnan[1,3], Edoardo Borgomeo[1], Kasia Paprocki[4], M. Shah Alam Khan[5], Mashfiqus Salehin[5], and Jim W. Hall[1].

[1]School of Geography and the Environment, University of Oxford, United Kingdom

[2]Commonwealth Scientific and Industrial Research Organisation, Australia

[3]Department of Urban and Regional Planning, Chittagong University of Engineering and Technology, Bangladesh

[4]London School of Economics and Political Science, United Kingdom

[5]Bangladesh University of Engineering and Technology, Bangladesh

Corresponding author: Emily J Barbour, Commonwealth Scientific and Industrial Research Organisation, Australia; emily.barbour@csiro.au; +61 (2) 6246 5992

Supplementary Information

This document provides a summary of the main model components. Building on the conceptual model described in Borgomeo et al. [1], we represent the following main processes: flooding, embankment reliability, salinity, waterlogging, farm holdings and crop yield. A summary of model performance and optimisation results is also provided. Figures were generated using R with the following libraries: ggplot2, reshape, ggpubr, egg, and readx1.

Flooding

Flood frequency and magnitude are estimated using Landsat satellite images from 1988 to 2012. Flood events are filtered using regional averaged river and surge level data, to include only those caused by fluvial-tidal or storm surge flooding (as opposed to pluvial flooding caused by monsoon precipitation) (Supplementary Figure 1). Storm surge floods include those caused by Cyclone Sidr in 2007, Cyclone Aila in 2009, and non-cyclonic storms from monsoon depressions [2]. Methods for estimating the size and timing of events are described in Adnan et al. [2], and are applied here specifically for the six case study polders. Estimates are likely to be an underestimation, as they are based on pre- and post-monsoon satellite imagery due to cloud obscuring the images during the monsoon. However, they provide the best available evidence of the frequency and magnitude of events across the case study polders.

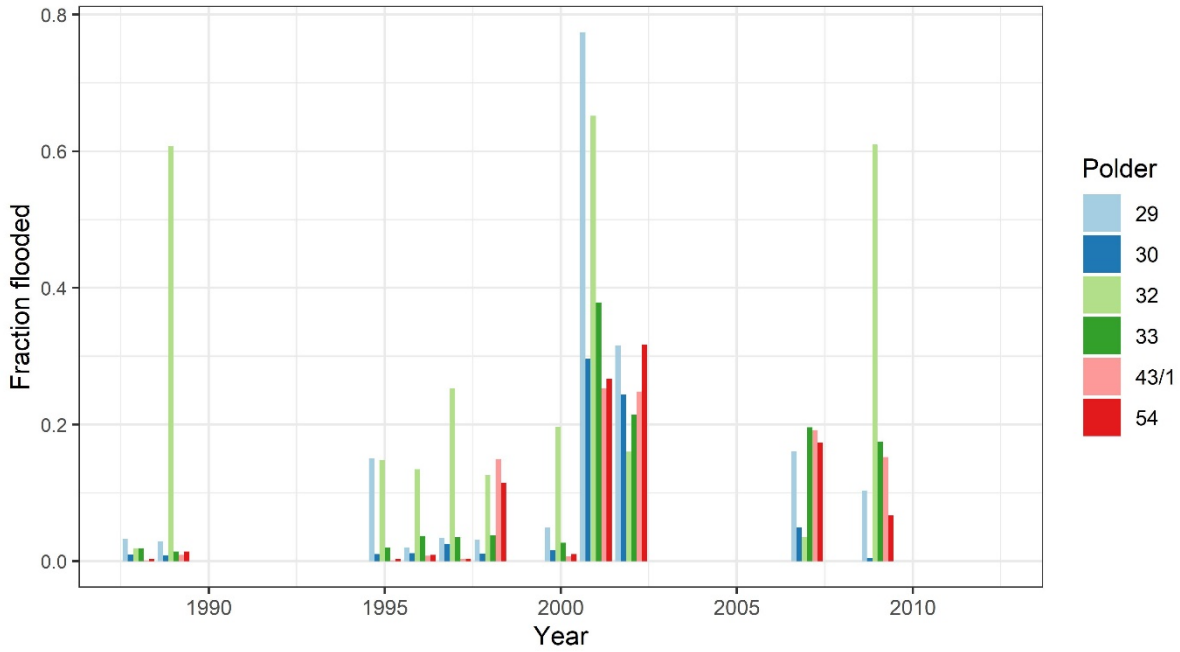

Supplementary Figure 1. Observed fraction flooded for the six polders between 1988 and 2012 based on fluvial-tidal and/or storm surge events.

Water level data at Dumuria, Chalna and Mongla were also analysed, along with observed cyclone events. However, there was no clear relationship with observed area flooded. This points to complex mechanisms influencing flood inundation inside the polders, with flooding often due to a combination of elevated water levels, storm events, and deteriorated embankments resulting in breaching [2,3]. Breaching is reported to be the more frequent cause of inundation compared with overtopping, hence may not necessarily coincide with the highest water levels. Spatial resolution

and uncertainty in observed data also contributes to difficulty in attributing observed flooding to specific driving mechanisms.

This combination of drivers paired with lack of data on embankment breaching limits the capacity to calibrate modelled and observed flood events. Here, we calibrate flood magnitude and frequency by comparing modelled and observed fraction flooded. We note that the fraction flooded is dependent on embankment condition, which was not included in the calibration due to lack of information.

Using observed data, flood frequency was defined using a Poisson distribution with λ=1/27 (one event in just over two years, with 27 being months), whilst flood magnitude was calibrated to give the following values for the *a* and *b* parameters of the beta distribution (see Borgomeo et al. [1] for details regarding these distributions): (1) *a* parameter: 0.9, 0.8, 1.0, 0.8, 0.5, and 0.7; and (2) *b* parameter: 2.9, 8.4, 1.8, 8.3, 7.8 and 8.0 for polders 29, 30, 32, 33, 43/1 and 54 respectively.

A Quantile-Quantile plot comparing modelled with observed events run using 10,000 years of model simulation is shown in Supplementary Figure 2. There is a poor fit for small to medium events with the model underestimating observations. The fit is poorer for polders with fewer flood events, and is also biased toward fitting larger events based on the calibration objective function. This is expected given only 11 observed events were available for calibration. The calibration assumed a constant embankment condition of 0.6 for all polders. Not surprisingly, the calibration was highly sensitive to this assumption for lower condition values given the condition directly influences frequency and magnitude of inundation.

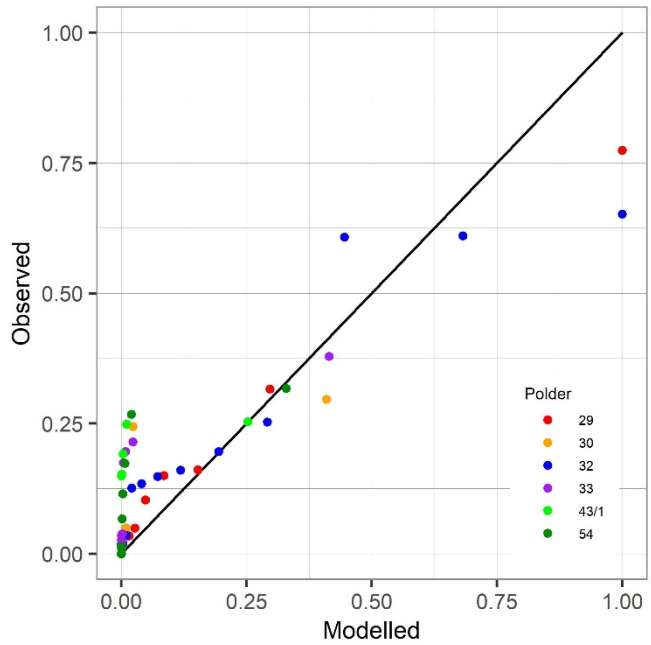

Supplementary Figure 2. Quantile-Quantile plot comparing modelled and observed fraction flooded for the six polders (red=Polder 29, orange=Polder 30, blue=Polder 32, purple=Polder 33, light green=Polder 43/1, and dark green=Polder 54) using calibrated beta and lambda values. Simulations are run for 10,000 years.

The stochastic generation of flood events does not account for seasonality. Whilst this is significant in Bangladesh given most fluvial-tidal events occur during the monsoon, the observed flood events between 1988 and 2012 occurred throughout the year (May, July,

August, September, October and November, Supplementary Figure 1). Major cyclones SIDR and Aila occurred in November and May respectively.

The analysis is focussed upon a baseline condition, which includes endogenous changes to the system, for example due to embankment deterioration, but does not yet incorporate exogenous changes in future flooding due to factors such as climate change, sea level rise, or changed sediment supply to the delta. Analysing the system's sensitivity to these factors will be the subject of future research. We do consider increases in flooding due to embankment deterioration, being our main focus of analysis and the main cause of increased flooding [2,4,5].

Having generated a series of flood events for each polder, we then calculate the fraction flooded within the polder, which is subsequently used to identify which mauzas, the smallest administrative unit, (if any) are considered to be flooded based on elevation. The fraction flooded (F_F) for polder p at time t is calculated in a manner similar to that used by Borogmeo et al. [1] (we exclude an additional damage parameter used in Borgomeo et al.):

$$F_F(p,t) = \begin{cases} \dfrac{1}{e_R(p,t)} \cdot f^3(p,\tau) & \text{if } t = \tau \\ \left(\dfrac{1}{e_R(p,t)} \cdot f^3(p,\tau) \right) \cdot e^{-\frac{\tau - t}{5}} & \text{if } \tau < t < \tau + 5 \end{cases}$$

Fraction flooded is a function of the embankment reliability e_R and size of the flood event external to the polder (f) and starts at time $\tau = t$. It is then assumed that the flood recession follows an exponential decay over six months.

The average elevation is then estimated for each entire polder (L_P) and that of each mauza (L_M) using the Shuttle Radar Topography Mission (SRTM) digital elevation model [6]. Elevation bands are defined for each polder, and assigned to each mauza (Supplementary Table *1*). During a flood, any mauza where $L_M < L_P$ is assumed to be flooded.

Supplementary Table 1. Elevation bands derived using SRTM

Elevation Band (m)	Polder 29		Polder 30		Polder 32		Polder 33		Polder 43/1		Polder 54	
	Cumul. %	No. Mauza	Cumul. %	No. Mauza	Cumul %	No. Mauza	Cumul. %	No. Mauza	Cumul. %	No. Mauza	Cumul. %	No. Mauza
-8 - 2	23	0	22	0	46	0	15	0	5	0	2	0
2 - 3	51	21	51	5	64	3	46	0	13	0	8	0
3 - 4	73	30	75	22	84	2	75	7	29	0	22	0
4 - 5	83	17	88	9	94	1	90	2	49	1	45	1
5 - 6	89	5	94	0	98	0	96	0	68	25	67	12
6 - 7	94	0	98	0	100	0	99	0	83	10	83	6
7 - 8	97	0	99	0	100	0	100	0	92	2	92	0
8 - 9	99	0	100	0	100	0	100	0	97	2	97	0
9 - 23	100	0	100	0	100	0	100	0	100	1	100	0

Embankment reliability

Embankment deterioration was modelled as described by Borgomeo et al. [1], with deterioration rates unchanged for Polder 54 (0.005), and halved for the remaining polders (0.0025). The higher

deterioration for Polder 54 is based on observed erosion maps showing higher rates in this region [7]. At these rates, the embankment condition deteriorates to 0.1 after 29 years (with a starting condition of 0.6 for all polders in the absence of any rehabilitation or flood events – representative of 60% of the maximum condition). Values are estimated given the absence of actual embankment deterioration. Further analysis of erosion data (unavailable for this study) and impacts on embankments would be needed to improve this estimate.

Salinity

Different initial soil salinity concentrations are used to reflect spatial across the polders. Polder-scale concentrations are estimated using Upazila-scale data [8] using an area weighted average of different salinity categories (Supplementary Figure 3 and Supplementary Table *2*). Historical salinity values are also estimated for 60 years prior to 2009 (from 1949 to 2009) by back-casting using the same historical rate of change, and are used to evaluate model performance. Rate of change is estimated by fitting a linear trend to observed data and averaging across the three Upazilas (Supplementary Figure 4). Assumed river salinity values are shown in Supplementary Table *3*. For both soil and river salinity, time-series data was not available.

The persistence of elevated salt concentration following a flood event was estimated in the absence of further information to decline by roughly 50% over a period of two years. Clarke et al. [9] found irrigation water at 8 ppt (approximately 10-15 dS/m) to result in the persistence of modelled elevated salt concentrations for 65% of the 118 years of simulation.

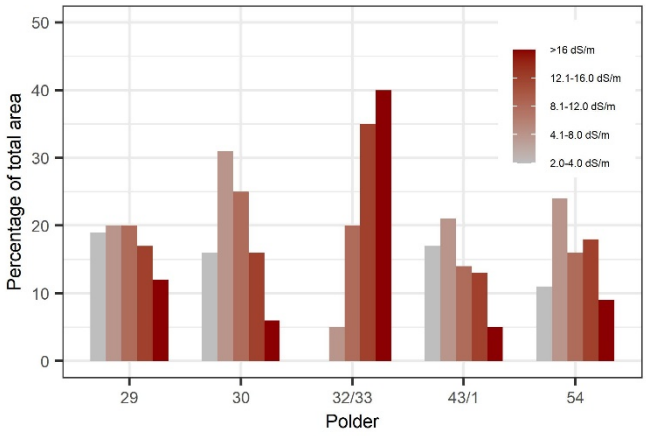

Supplementary Figure 3. 2009 soil salinity categories for the case study polders with percentage area for each polder (Source: derived using data from Soil Resources Development Institute, 2010).

Supplementary Table 2. Estimated average soil salinity for current and historical simulations based on data from SRDI [8]

	Polder					
	29	**30**	**32**	**33**	**43/1**	**54**
Average salinity (2009) (dS/m)	9	9	14	14	8	9
Estimated historical salinity	4	3	8	8	3	4

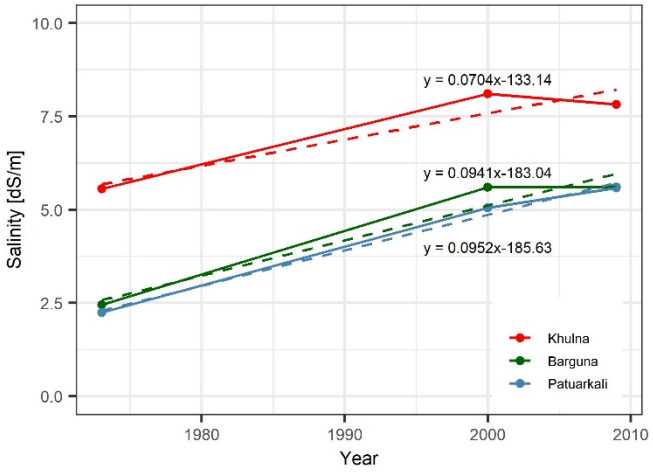

Supplementary Figure 4. Temporal change in salinity with the average estimated as being +0.09 dS/m per year.

Supplementary Table 3. Assumed river salinity for each polder, used to for model parameter s_R (derived from SRDI [8]).

	Polder					
	29	**30**	**32**	**33**	**43/1**	**54**
Station	**Dumuria**	**Batiaghata**	**Dacope**	**Dacope**	**Barguna (Amtali) - Payra river**	**Kalapara**
River salinity (dS/m)	17	28	28	28	2	28

*assume same as for Batiaghata

Waterlogging

River levels used for modelling waterlogging are estimated using average observed water level data for three stations in the South West zone (SW 28 - Dumuria, SW 244 - Mongla, and SW 243 - Chalna) [10]. There is insufficient spatial resolution in available data to show variations between polders. Levels are a monthly average of the maximum monthly high tide value from April 1982 to February 2003.

The rate of deterioration of drainage infrastructure (which influences waterlogging) is set to 0.005 [1]. Using a starting condition of 0.8 (on a scale of 0 to 1 with 1 being completely functional), this results in a deterioration of 50% in approximately 10 years, reaching close to zero (0.02) in approximately 60 years (period of simulation). Similar to embankment deterioration, this is estimated in the absence of observed data. A 1993 Bangladesh Southwest Area Water Resources Management Plan [11] states that the six case study polders had satisfactory polder drainage (with less than 30% of area experiencing congestion) at the time, giving an indicative starting condition.

Farm holdings

The primary livelihoods in the study area are estimated based on a scoping visit of polders 29, 30, 32, 33 and 35/3 [12], and are reported as being: agriculture/aquaculture; day labourers (including temporary migration to urban areas in search of work); fishing (including fish fry collection although this has been restricted through government embargos); some small service oriented business; and professional occupations (such as teachers and NGOs). High levels of unemployment are reported in

some areas of Polder 32. Many women work as housewives in non-income generating roles. This is consistent with the livelihood categories for south western and central Bangladesh adopted by Lazar et al. [13]. Whilst the focus of this analysis is on agriculture, it could be extended to consider other livelihood types.

The use of non-farm holdings to represent subsistence farmers is intended to capture the differential impacts on poorer households. It is recognised that there is significant potential to further extend this to consider a greater diversity in income and labour, as well as the landless poor.

A summary of the four categories of income groups is shown in Supplementary Table 4, and is implemented at a mauza scale to enable intra-polder variability in income to be modelled. Small farms dominate the study area. Available information on gender disaggregation based on household head for holdings and population engaged in agricultural work is shown in Supplementary Table 5.

Supplementary Table 4. Farm size characteristics and holdings by polder, estimated using agricultural census data [14].

Type	Area (acre) (average shown in brackets)	Area (ha)	No. Holdings by Polder					
			29	30	32	33	43/1	54
Subsistence (non-farm holding with cultivated area)*	<= 0.04 (0.02)	0.01	910	355	960	1,110	1,678	1,035
Small farms	0.05 – 2.49 (1.27)	0.51	7,502	4,699	3,828	6,798	10,511	4,655
Medium farms	2.5 – 7.49 (5.0)	2.0	1,946	1,568	1,005	1,882	3,382	2,142
Large farms	7.50 – 25+ (16.25)	6.6	215	178	242	299	570	411
Total holdings			***10,573***	***6,800***	***6,035***	***10,089***	***16,141***	***8,243***
Total area (ha)			***9,146***	***6,711***	***5,569***	***9,215***	***15,903***	***9,381***

**Non-farm holdings with cultivated area was estimated using the total non-farm holdings at a mauza scale, and the proportion of non-farm holdings with cultivated area at an Upazila scale (not available at a mauza scale).*

Supplementary Table 5. Gender differences in farm holdings and agricultural work for Upazilas Dumuria (Polder 29), Batiaghata (Polder 30), Dacope (Polders 32 and 33), Amtali (Polder 43/1) and Kala Para (Polder 54) [14].

Holding Type	Farm holding head (%)		Population engaged in agricultural work (%)	
	Male	Female	Male	Female
Subsistence (non-farm holding with cultivated area)	95	5	68	32
Small farms	98	2	71	29
Medium farms	99	1	74	26
Large farms	99	1	77	23

Crop yield

Yearly (y) crop yield is calculated as the monthly minimum yield for each year to account for salinity, waterlogging and flood impacts. Winter crops which span a calendar year are therefore misrepresented, but given yields are averaged over all years and stochastic simulations, this is unlikely to have a significant impact on results. Production per crop and holding type ($P_{x,h}$) is

$$P_{x,h}(y) = \min Y_x(t) \cdot r_x \cdot A_h \cdot N_h \cdot$$

Mauza scale differences in cropping patterns were considered, but have a higher level of uncertainty than Upazila differences given lack of available data and the higher likelihood for them to change over time. Differences between small, medium and large farm holdings are minimal based on data from Khulna Upazila. Cropping patterns for each polder are estimated by selecting the largest Upazila which overlaps.

Based on available agricultural census data [14], major crops for the Upazilas covering our case study polders included aus, aman, boro, jute, oil seeds and pulses. We focus here on aus, aman, boro and jute given these are considered major crops (along with potato and wheat) [15]. Wheat was not present in the mauzas for our study area based on available data. Oil seeds and pulses are an aggregate of multiple crops and hence are also not included.

In the absence of additional information, vegetable growing for subsistence farmers is represented using water gourd and pumpkin (winter and summer). The actual yield for subsistence farmers is not known, hence the census data for farm holdings is used as an approximation. The actual yield is therefore likely to be lower than indicated here.

Crop differences in yield sensitivity to salinity is not captured in this model, and could be included in future work.

Crop prices are based on average values from agricultural census data [15], which can differ from local prices. We assume an exchange rate of 1 taka = 0.0116 USD at the time of writing.

Supplementary Table 6. Crop characteristics

Crop	Potential yield (t/ha)[1]	Crop price (taka/kg)[2]	Crop calendar[3]	Subsistence	Small	Medium	Large
Local Aus	2.5	13.4	Apr-Aug		X	X	X
HYV Aus	5.5	13.2	Apr-Aug		X	X	X
Local Aman	2.5	13.7	Aug-Dec		X	X	X
HYV Aman	5.5	15.7	Aug-Dec		X	X	X
Local Boro	2.5	14.3	Nov-May		X	X	X
Hybrid Boro	10	16.2	Jan-May		X	X	X
HYV Boro	7	16.2	Jan-May		X	X	X
Jute **(bales)**[4]	15	8557	May-Sep		X	X	X
Water gourd	28	13.3	Jul-Mar	X			
Pumpkin (winter, Rabi)	35	13.2	Nov-Mar	X			
Pumpkin (summer, kharif)	35	13.2	Mar-Nov	X			

[1]Values taken from a combination of data and expert knowledge [16]. The value for pumpkin is based on BARI Mistikumra-1, early winter variety [17].

[2]From Yearbook of Agricultural Statistics 2016 [15] Table 10.3. Prices quoted as per quintal taka with the assumption that 1 quintal = 100kg. No price was included for hybrid boro hence values for HYV boro were used as an approximation.

[3] Crop calendars are given as ranges using information from Yearbook of Agricultural Statistics 2016 [15]. Here, months are taken to be the widest range, whilst in reality the growing season is likely to be shorter. However, given these calculations are focused on the maximum flood area during the season, this is unlikely to have a significant impact. Dates for pumpkin were not given, hence were estimated using data on kharif and rabi seasons.

[4]Jute is reported in bales, where 1 bale=180kg. Values are consequently reported for bales/ha and taka/bale.

Model performance

Model performance is evaluated by comparing against observed District-scale crop yields in Khulna (Polders 29, 30, 32 and 33), Barguna (Polder 43/1) and Patuarkhali (Polder 54) (Supplementary Figure 6). The comparison is limited by differences in the spatial scale of observed data (District) compared with modelled (polder), as well as limitations in comparable dates and crops. We used District-scale observed data for all crops for 2014/2015 and 2015/2016 BBS[15]. We also use observed yields from 2001/2002 to 2009/2010 [18], although the available data only included local and HYV aus, HYV aman, and local and HYV boro for Khulna and Pautarkhali. Modelled results draw on observed Upazila-scale cropping patterns and mauza-scale numbers of farm holdings.

We use a 60-year modelled 'historical scenario' to provide a more realistic comparison with observed historical data. This is configured using higher starting elevations (adding 1m based on observations from Auerbach et al. [5] for unpoldered areas), combined with lower starting soil salinity levels (see salinity section for values) from 1949-2009. 1000 stochastic simulations are used to evaluate variability across different stochastic flood events.

The ranges in modelled and observed data are presented as box plots to reflect both availability and uncertainty in data.

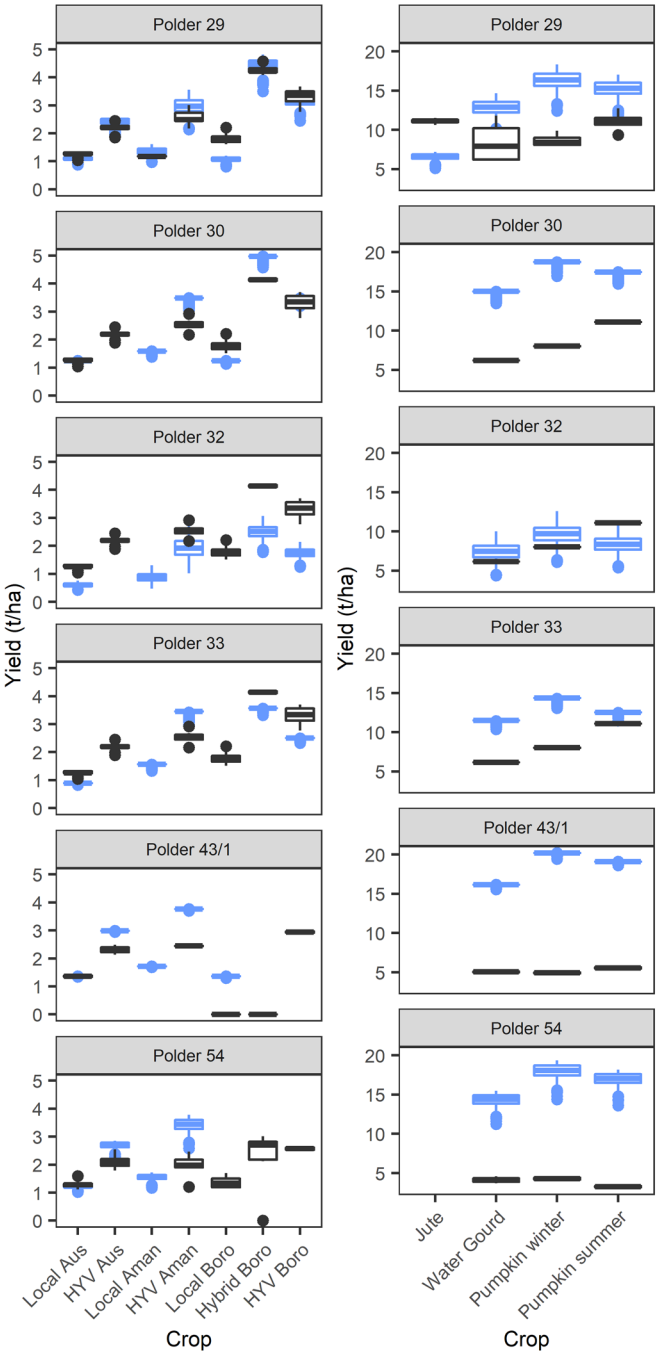

Supplementary Figure 5. Comparison between observed (black) and modelled (blue) crop yields. Observed data from BBS Yearbooks from 2001/2002 to 2009/2010 for local and HYV Aus, HYV Aman, Local and HYV Boro, (Khulna and Patuarkhali); and 2014/2015 and 2015/2016 for all crops except Local Aman (all Upazilas). The modelled data uses the 'historical' scenario with increased elevation and reduced soil salinity across 1000 stochastic simulations. Observed data includes 462 data points in total with variations between years and crops. Box plots include the median, two hinges (first and third quartiles), two whiskers (representing values up to 1.5x the inter-quartile range), and individual outlying points.

There is substantial variation in performance between crops and polders, with the lower yield crops (rice) generally performing better than the higher yield crops (jute, water gourd and pumpkin) with the exception of Polder 32 (Supplementary Figure 6). In some locations, yields are shown as non-zero in the District level observed data, yet are reported as not being grown based on Upazila-scale cropping patterns (such as HYV aus for Polder 30).

For most polders, the modelled yields for vegetables for subsistence farmers are substantially higher than observations (noting that observations are for all farm holdings and not for subsistence farmers), suggesting that crop losses are far greater than for rice. Better agreement is observed in Polders 29 and 32 where there is a higher incidence of flooding. This suggests there may be additional significant factors decreasing crop yield that are either not considered here, for example pests or access to fertiliser. However, without any specific data for local yields on subsistence farms, it is difficult to determine whether our model does over-estimate yields. Should it do so, it is likely that crop income for subsistence farmers is lower still than estimated here.

We note the challenge in both calibrating and evaluating model performance in the representation of complex systems with poor data availability. Despite the mixed performance across crops and polders, we believe the model provides valuable insights into the interaction of water-related risks across a highly heterogeneous region that can assist water infrastructure planning.

Embankment Investment Costs

Major investment projects targeting rehabilitation of the coastal embankment and drainage system are shown in Supplementary Table 7. Our estimated cost of $204 million USD to rehabilitate the six case study polders draws on our own calculations using polder lengths and estimated costs for existing projects [23], and hence should not be taken to reflect actual detailed costings of embankment rehabilitation.

Supplementary Table 7. Embankment rehabilitation project costs

Project	Cost (million USD)
Coastal Embankment Rehabilitation Project	53 [19]
Khulna-Jessore Drainage Rehabilitation Project	45 [20]
Emergency 2007 Cyclone Recovery and Restoration Project	109 [21]
Coastal Embankment Improvement Project	400 [22]

Optimisation

A multi-objective optimisation algorithm eMoga [24] was used to explore trade-offs. eMoga has been previously applied in hydrological applications [25]. The algorithm parameter values used are shown in Supplementary Table 8.

Supplementary Table 8. eMoga parameter values

Parameter	Parameter value
Population	100
Maximum generations	10,000
Probability of crossover	1.0
Probability of mutation	0.003

Supplementary Figures

Polder flooding

Variations in flood events across the polders for a no embankment investment and high embankment investment scenario (using the single objective optimisation solution to minimise crop income loss) is shown in Supplementary Figure 6. The greatest flooding in Polders 32 and 29 is consistent with observed data reported by Adnan et al. [2]. Using 1000 stochastic simulations, results show variability in the magnitude and frequency of events, yet the overall pattern of flooding between the polders is unchanged. The number of large flood events reduces under a high embankment investment scenario.

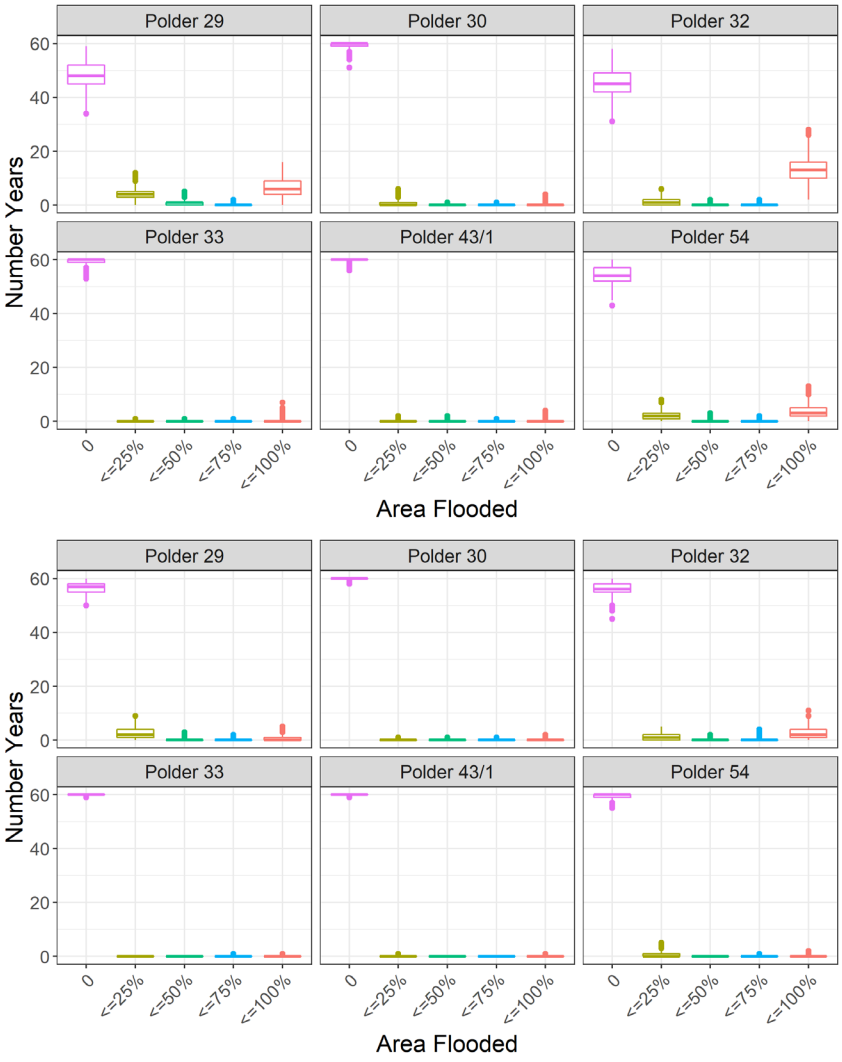

Supplementary Figure 6. Number of years during the sixty-year simulation that experience internal flooding of different magnitude, shown as a percentage of the total polder area. A high embankment investment scenario (bottom plot) shows limited improvement in area flooded compared with a no investment scenario (top plot). Box plots show the variation across 1000 stochastic simulations and include the median, two hinges (first and third quartiles), two whiskers (representing values up to 1.5x the inter-quartile range), and individual outlying points.

Crop Production

With no embankment investment for a single model iteration, total crop production is greatest in Polders 29 (with more high yield crop varieties) and 43/1 (with the greatest crop area), and smallest in Polder 32 and 30 (which have the smallest crop area) [14].

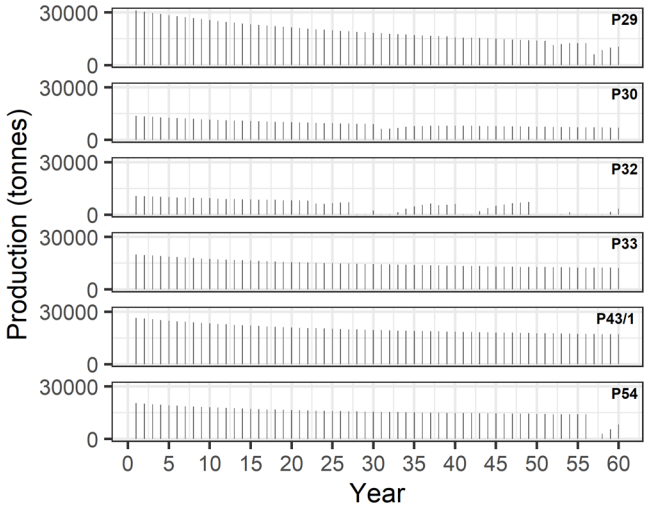

Supplementary Figure 7. Total crop production for each polder during the sixty-year simulation assuming no embankment investment.

Optimisation

The following figures show variations in embankment investment timing and frequency for:

1. Single objective optimisation to minimise expected crop income loss, $\min E(L)$;
2. Single objective optimisation to minimise expected crop income loss with a $200 million USD constraint on investment, $\min E(L)$ subject to $TIn = \sum_{p=1}^{P}\sum_{r=1}^{R} In_{p,r} \leq 200 \text{ million USD}$ (where P are the six polders, R is the number of embankment rehabilitation investments over the simulation for each polder, and In is the investment cost); and
3. Multi-objective optimisation to minimise expected crop income loss and total investment cost.

In all cases, loss is calculated for each farm holding type (subsistence, small, medium and large, h) as a sum of crop income over all polders and crops (C), and averaged over the 60 year simulation (T):

$$L_h = \sum_{p=1}^{P} \frac{\sum_{c=1}^{C} \bar{I}_{p,h,c} - \sum_{t=1}^{T}\sum_{c=1}^{C} \frac{I_{p,h,c}}{T}}{\sum_{c=1}^{C} \bar{I}_{p,h,c}}$$

Expected loss is calculated as: $E(L_h) = \sum_{n=1}^{N} \frac{L_h}{N}$ by averaging over the number of stochastic simulations (N=100). Each of the three optimisations above are repeated for all household types in aggregate where $E(L) = \sum_{h=1}^{H} E(L_h)$; or for subsistence farmers only: $E(L) = E(L_{subsistence})$.

1. Minimising expected crop income loss

The sequence of embankment rehabilitation investments allowing the maximum of three for each polder is shown in Supplementary Figure 8. A column shows when an investment is made, with the y-axis showing the year of investment. Investments are spread across the investment period with minimal differences in timing.

Two epsilon values (used to define the resolution of the non-dominated solution space) were tested for the loss objective function, the first being 0.1 and the second being 0.01 to allow greater resolution for archived non-dominated solutions. However, differences in modelled loss were insignificant (0.555 for an epsilon value of 0.1 and 0.556 for an epsilon value of 0.01). A further epsilon value test using 0.001 was used for the no waterlogging/no salinity scenario, and similarly had no significant impact.

Differences between the with and without waterlogging/salinity scenarios, and between optimising for all farm holdings compared with only subsistence farmers had little impact on the investment strategy. Removing waterlogging and salinity significantly reduced the expected crop income loss. Losses for subsistence farmers only are higher than those averaged across all four farm holding types.

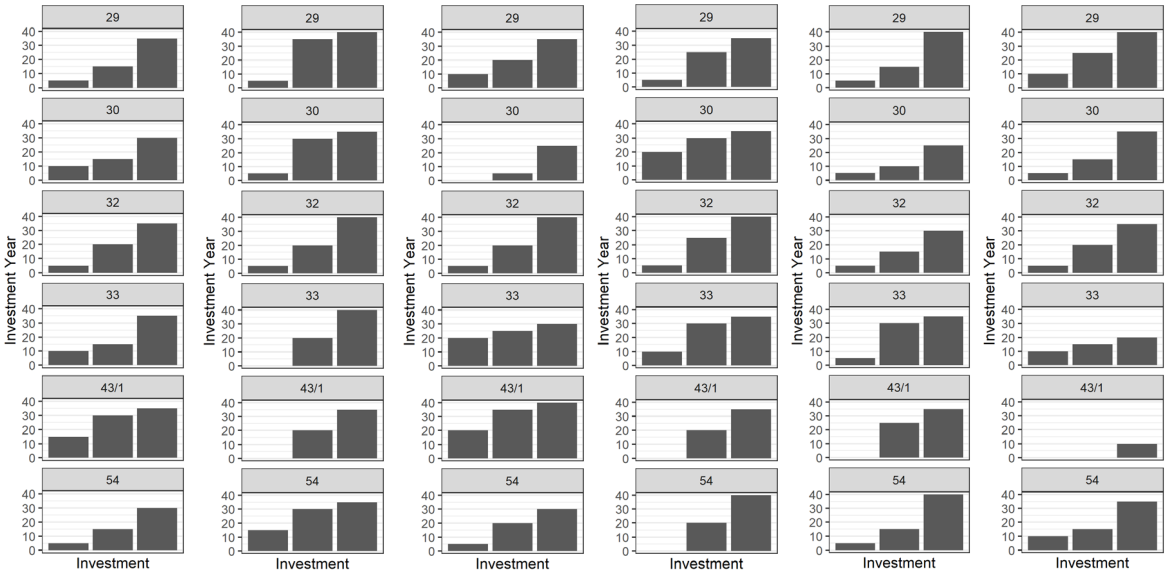

Supplementary Figure 8. Optimisation investments for single objective with no constraint. Left to right: all farm holdings (epsilon value = 0.1); all farm holdings with epsilon value = 0.01; all farm holdings with no salinity or waterlogging and epsilon value of 0.01; all farm holdings with no salinity or waterlogging and epsilon value of 0.001; subsistence only (epsilon of 0.1); subsistence only (epsilon value of 0.01). Average loss L to R: 0.555; 0.556; 0.004; 0.004; 0.699; 0.699.

2. Minimising expected crop income loss with cost constraint

When a cost constraint is introduced, clear differences in investment priority between polders are observed (Supplementary Figure 9). The greatest investment is in Polders 32 and 54 with no investment in Polders 33 and 43/1. The exact timing is found to be sensitive to variations in stochastic events and optimisation performance, tested by repeating the optimisation three times as a sensitivity test.

Removal of waterlogging and salinity did not have a significant impact on investment strategy, with differences between sensitivity runs being similar or greater than differences between the with and without waterlogging/salinity scenarios. Losses are significantly reduced. Similarly, optimising for subsistence farmers only has no observable impact on investment strategy.

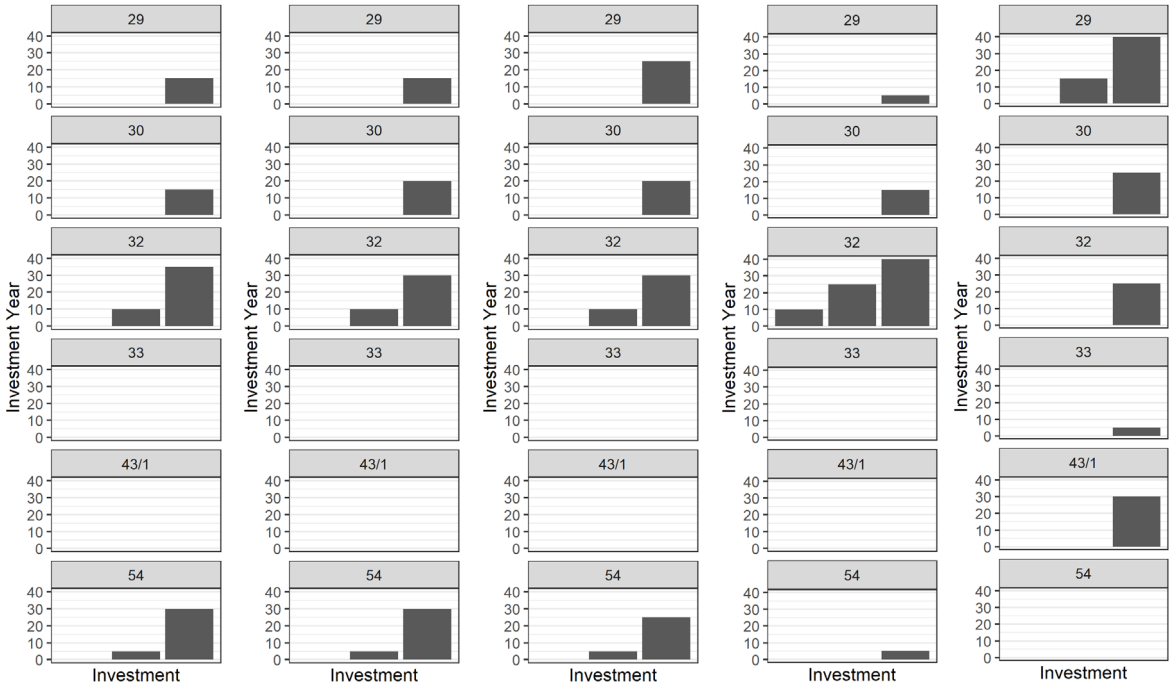

Supplementary Figure 9. Optimisation investments for single objective (all farm holdings) with a $200 USD constraint. Left to right: epsilon value of 0.1; epsilon value of 0.01; sensitivity test 1; sensitivity test 2; sensitivity test 3. All sensitivity tests use and epsilon value of 0.01. Average loss L to R: 0.559; 0.559; 0.559; 0.560; 0.569.

3. Minimising expected crop income losses and investment cost

When both crop income loss and investment cost are minimised using multi-objective optimisation, there is consistently no investment in Polder 43/1 across all non-dominated solutions, with the highest investment in Polder 32 followed by Polder 29 (Supplementary Figure 10). Overall, there are very few non-dominated solutions suggesting a lack of sensitivity of crop loss to embankment investments and consequently flooding (Supplementary Figure 11). This can also be seen from the small change in loss despite changes in the number of investments. The solutions are sensitive to the stochastic simulation of the flood events and the optimisation performance, with a lower loss found using multi-objective optimisation (with 9 investments in total) compared with a single objective (using 16 investments).

Consistent with the single objective optimisation results, removal of waterlogging and salinity as well as optimising for subsistence farmers only has no significant impact on investment strategy, yet changes the resulting expected crop income loss (Supplementary Figure 11).

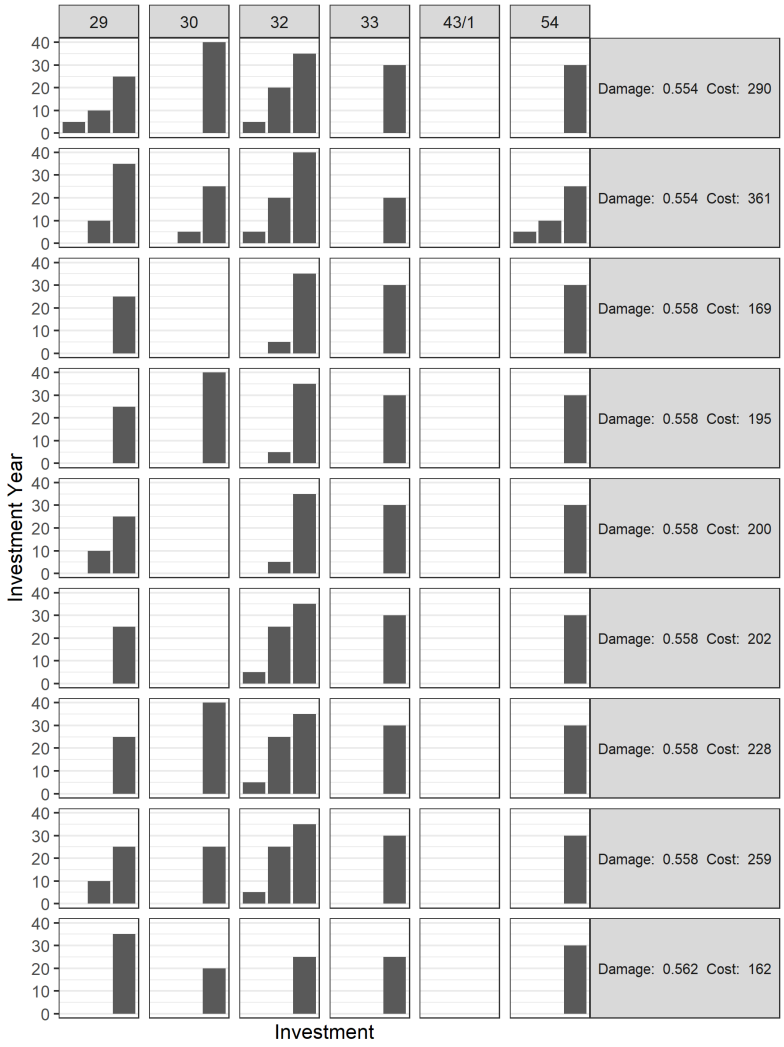

Supplementary Figure 10. *Optimisation investments for two objectives (minimise crop income loss and investment cost) for all farm holdings (epsilon value of 0.01 for loss and 1.0 for investment cost).*

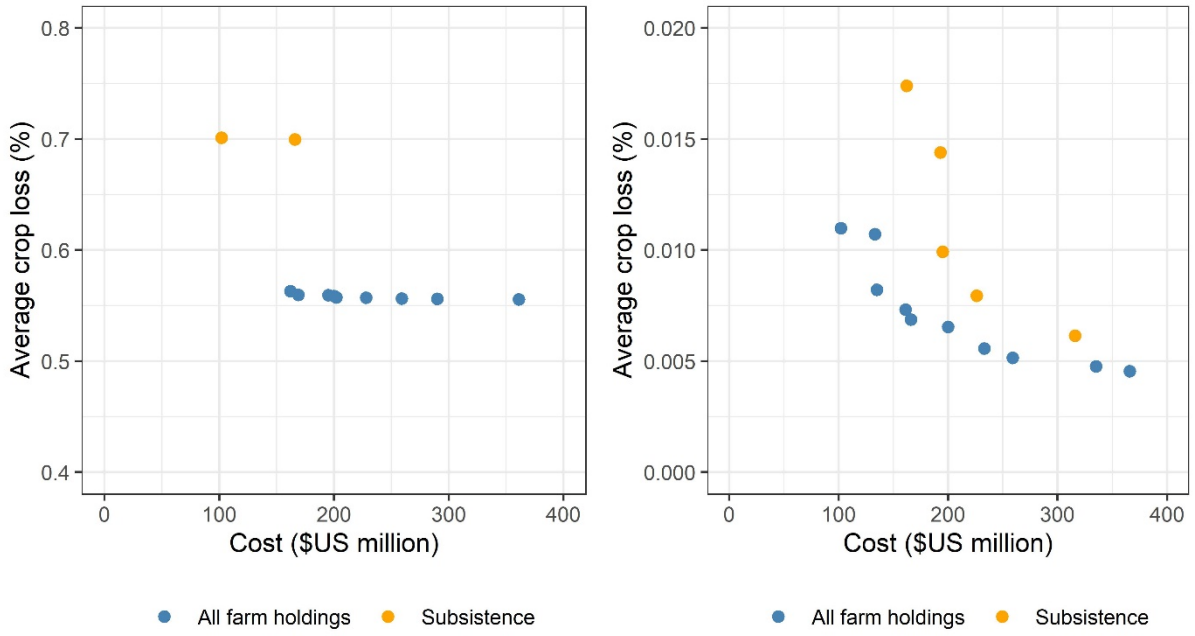

Supplementary Figure 11. Non-dominated multi-objective optimisation solutions for all farm holdings and subsistence farmers only with L: salinity and waterlogging included; and R: removed. With salinity and waterlogging, loss is close to 70% for subsistence farmers, as opposed to ~55% averaged across all farm holdings. Without salinity and waterlogging, loss is less than 2%. In both cases, loss is relatively insensitive to investment.

References

1 Borgomeo, E., Hall, J. W. & Salehin, M. Avoiding the water-poverty trap: insights from a conceptual human-water dynamical model for coastal Bangladesh. *International Journal of Water Resources Development* **34**, 900-922, doi:10.1080/07900627.2017.1331842 (2018).

2 Adnan, M. S. G., Haque, A. & Hall, J. W. Have coastal embankments reduced flooding in Bangladesh? *Science of The Total Environment* **682**, 405-416, doi:https://doi.org/10.1016/j.scitotenv.2019.05.048 (2019).

3 Islam, M. F., Bhattacharya, B. & Popescu, I. Flood risk assessment due to cyclone-induced dike breaching in coastal areas of Bangladesh. *Nat. Hazards Earth Syst. Sci.* **19**, 353-368, doi:10.5194/nhess-19-353-2019 (2019).

4 van Staveren, M. F., Warner, J. F. & Shah Alam Khan, M. Bringing in the tides. From closing down to opening up delta polders via Tidal River Management in the southwest delta of Bangladesh. *Water Policy* **19**, 147-164, doi:10.2166/wp.2016.029 (2016).

5 Auerbach, L. W. *et al.* Flood risk of natural and embanked landscapes on the Ganges–Brahmaputra tidal delta plain. *Nature Climate Change* **5**, 153-157, doi:10.1038/nclimate2472 (2015).

6 Farr, T. G. *et al.* The Shuttle Radar Topography Mission. *Reviews of Geophysics* **45**, doi:10.1029/2005rg000183 (2007).

7 *Erosion data for coastal Bangladesh* (DEltas, vulnerability and Climate Change: Migration and Adaptation (DECCMA), 2017).

8 *Saline Soils of Bangladesh* (Soil Resource Development Institute, SRMAF Project, Ministry of Agriculture, 2010).

9 Clarke, D., Williams, S., Jahiruddin, M., Parks, K. & Salehin, M. Projections of on-farm salinity in coastal Bangladesh. *Environmental Science: Processes & Impacts* **17**, 1127-1136, doi:10.1039/C4EM00682H (2015).

10 *Water Station Data SW 28 – Dumuria, SW 243 – Chalna, SW 244 Mongla* (Bangladesh Water Development Board, 2017).

11 *Flood Action Plan 4 (FAP 4). Southwest Area Water Resources Management Project, Final Report* (People's Republic of Bangladesh, Ministry of Irrigation, Water Development and Flood Control, 1993).

12 Uddin, M. S., Rahman, M. M., Sarkar, M. & Khan, M. B. U. Scoping Visit: Polder 29, 30, 32, 33, 35/3. Draft Report (Unpublished). (2016).

13 Lázár, A. N. *et al.* in *Ecosystem Services for Well-Being in Deltas: Integrated Assessment for Policy Analysis* (eds Robert J. Nicholls *et al.*) 525-574 (Springer International Publishing, 2018).

14 *Census of Agriculture 2008* (Bangladesh Bureau of Statistics, Planning Division, Ministry of Planning, Government of the People's Republic of Bangladesh, 2011).

15 *Yearbook of Agricultural Statistics-2016* (Bangladesh Bureau of Statistics, Statistics and Information Division, Ministry of Planning, Government of the People's Republic of Bangladesh, 2017).
16 Mainuddin, M. (2019). Personal Communication.
17 Chowdhury, M. A. H. & Hassan, M. S. Hand Book of Agricultural Technology. (Farmgate, Dhaka, 2013).
18 *Crop yield data from 2001/02 to 2009/10 collated from Bangladesh Bureau of Statistics Yearbooks of Agricultural Statistics* (Bangladesh Bureau of Statistics, Statistics and Information Division, Ministry of Planning, Government of the People's Republic of Bangladesh).
19 *Staff Appraisal Report Bangladesh: Coastal Embankment Rehabilitation Project* (The World Bank, 1995).
20 *Project Performance Evaluation Report in Bangladesh. Bangladesh: Khulna-Jessore Drainage Rehabilitation Project* (Asian Development Bank, 2007).
21 *Emergency 2007 Cyclone Recovery and Restoration Project (ECRRP)* (The World Bank, 2008).
22 *Project Information Document (PID) Appraisal Stage: Coastal Embankment Improvement Project - Phase 1 (CEIP-1)* (The World Bank, 2013).
23 *Development Project Proforma/Proposal (DPP) for Blue Gold Program (BWDB Component)* (Government of the People's Republic of Bangladesh, Ministry of Water Resources, Bangladesh Water Development Board, 2013).
24 Laumanns, M., Thiele, L., Deb, K. & Zitzler, E. Combining Convergence and Diversity in Evolutionary Multiobjective Optimization. *Evolutionary Computation* **10**, 263-282, doi:10.1162/106365602760234108 (2002).
25 Mortazavi-Naeini, M., Kuczera, G. & Cui, L. Efficient multi-objective optimization methods for computationally intensive urban water resources models. *Journal of Hydroinformatics* **17**, 36-55, doi:10.2166/hydro.2014.204 (2015).